Origins of optical absorption and emission lines in AlN

Qimin Yan, Anderson Janotti, Matthias Scheffler, and Chris G. Van de Walle

Citation: Applied Physics Letters **105**, 111104 (2014); doi: 10.1063/1.4895786
View online: http://dx.doi.org/10.1063/1.4895786
View Table of Contents: http://scitation.aip.org/content/aip/journal/apl/105/11?ver=pdfcov
Published by the AIP Publishing

Origins of optical absorption and emission lines in AlN

Qimin Yan,[1,2] Anderson Janotti,[1] Matthias Scheffler,[1,3] and Chris G. Van de Walle[1]
[1]*Materials Department, University of California, Santa Barbara, California 93106-5050, USA*
[2]*Molecular Foundry, Lawrence Berkeley National Laboratory, Berkeley, California 94720, USA*
[3]*Fritz-Haber-Institut der Max-Planck-Gesellschaft, Faradayweg 4–6, D-14195 Berlin, Germany*

(Received 5 June 2014; accepted 3 September 2014; published online 15 September 2014)

To aid the development of AlN-based optoelectronics, it is essential to identify the defects that cause unwanted light absorption and to minimize their impact. Using hybrid functional calculations, we investigate the role of native defects and their complexes with oxygen, a common impurity in AlN. We find that Al vacancies are the source of the absorption peak at 3.4 eV observed in irradiated samples and of the luminescence signals at 2.78 eV. The absorption peak at ~4.0 eV and higher, and luminescence signals around 3.2 and 3.6 eV observed in AlN samples with high oxygen concentrations are attributed to complexes of Al vacancies and oxygen impurities. We also propose a transition involving Al and N vacancies and oxygen impurities that may be a cause of the absorption band peaked at 2.9 eV. © *2014 AIP Publishing LLC*. [http://dx.doi.org/10.1063/1.4895786]

There has been great progress in the growth of high-quality bulk AlN crystals as substrates for deep-UV light-emitting devices.[1,2] Still, the UV transparency of the material remains an outstanding issue. Conspicuous optical absorption bands in the blue and UV range are typically observed, and nearly all AlN crystals exhibit a yellow or dark amber color due to the presence of defects. It has been widely recognized that oxygen is the main impurity that contaminates the AlN crystals, and it has been suggested that the incorporation of oxygen is accompanied by the formation of Al vacancies.[3] Recent positron annihilation studies suggested that complexes of Al vacancies and oxygen on a nitrogen site (V_{Al}-O_N; see Fig. 1) are the dominant form of V_{Al} in as-grown AlN samples, whereas isolated V_{Al} was detected in irradiated samples.[4] In addition, defects on the nitrogen sublattice (either O_N or V_N) have been observed by electron paramagnetic resonance (EPR).[5,6] All these defects are expected to introduce defect states in the band gap of AlN (which is 6.2 eV wide); they may cause sub-band-gap light absorption that can interfere with the operation of optoelectronic devices. Despite these initial assignments, an explanation of the various experimental results based on detailed microscopic mechanisms has yet to emerge.

Broad peaks in the blue and UV range have also been observed in the absorption spectra of AlN layers synthesized under various growth conditions including metal organic chemical vapor deposition, NH_3-source molecular beam epitaxy, and physical vapor transport. A broad absorption band centered around 2.9 eV is frequently observed in as-grown AlN samples containing oxygen,[7–10] and a correlation between the yellow coloration and this absorption band has been established.[8] A variety of origins have been proposed for this 2.9 eV absorption band, including nitrogen vacancies,[7,8] Al interstitials,[11] and Al vacancies.[12] No reliable physical model has been offered for how these defects would give rise to this absorption band. Several other absorption bands have been observed for which the origins are also unknown: a peak at ~3.4 eV has been observed in irradiated AlN samples,[4,13] another centered around 4.0 eV (whose peak position slightly varies from sample to sample), and some other absorption bands in the range from 4 eV to 5.5 eV.[8,9] The 3.4 eV absorption band was tentatively attributed to nitrogen vacancies;[13] however, both Al and N vacancies can be generated by irradiation, and Al vacancies cannot be ruled out.

In addition to absorption spectra, AlN also exhibits a rich set of luminescence peaks. A luminescence band centered around 3.1–3.3 eV has been frequently observed in oxygen-containing samples.[14–16] Another luminescence band centered around 2.8 eV was reported in AlN samples with oxygen concentration around 2×10^{18} cm^{-3}; it was tentatively attributed to isolated V_{Al}.[12] Besides these two emission bands, a 3.6 eV luminescence band is frequently observed in bulk AlN with high oxygen concentration.[17,18] This emission peak has been previously attributed by Schulz *et al.*[19] to aluminum vacancies or its complexes. Calculations based on density functional theory (DFT) for native defects and related complexes in AlN have also been reported.[20–25] However, the severe underestimation of band gaps in DFT within the standard local-density or generalized gradient approximations[20–24] precluded a direct comparison of the calculated defect levels with the observed absorption or emission peaks. Recent advances in defect calculations based on the hybrid functional approach provide a more reliable description of defect levels in AlN.[25]

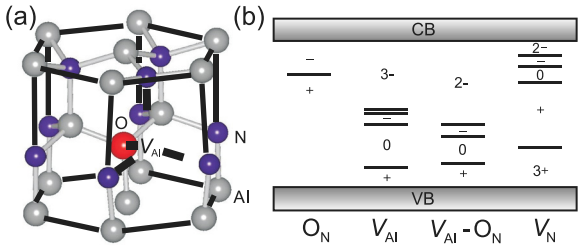

FIG. 1. (a) Geometry of the $(V_{Al}$-$O_N)^{2-}$ complex. Dashed lines are drawn between the nearest neighbors and the position of the missing Al atom. (b) Thermodynamic transition levels obtained from formation energies for defects. The conduction and valence bands are denoted by CB and VB.

In this letter, we determine the formation energy, transition levels, and optical properties of defects in AlN using hybrid-functional calculations to address the band-gap problem in the traditional DFT approach. Earlier studies indicate that vacancies are one of the most relevant defects in AlN,[22,25] and that O is the most prevalent impurity.[9] We therefore focus on Al vacancies (V_{Al}), N vacancies (V_N), substitutional O (O_N), and complexes composed of an Al vacancy and O impurity (V_{Al}-O_N). The absorption and emission energies are extracted from the calculated configuration-coordinate diagrams. Our results indicate that V_{Al} is likely responsible for the absorption peak at 3.4 eV and emission at 2.8 eV observed in irradiated samples, whereas the absorption band at 3.4 eV and emission at 3.1–3.3 eV, commonly observed in samples containing high O concentrations, are attributed to V_{Al}-O_N.

The calculations are based on generalized Kohn-Sham theory,[26] projector augmented wave (PAW) potentials,[27,28] and the screened hybrid functional of Heyd, Scuseria, and Ernzerhof (HSE),[29,30] as implemented in the VASP code.[31] The mixing parameter for the Hartree-Fock exchange potential is set to 32%, which reproduces the experimental band gap for AlN. The defects are simulated using a 96-atom supercell, a cutoff of 400 eV for the plane-wave basis set, and a $2\times2\times2$ k-point mesh for the integrations over the Brillouin zone. Spin polarization is included.

Native defects and their complexes usually exist in different charge states, depending on the position of the Fermi level. The stability of a particular charge state depends on its formation energy. For example, the formation energy of the V_{Al}-O_N complex is given by

$$E^f[(V_{Al}\text{–}O_N)^q] = E_t[(V_{Al}\text{–}O_N)^q] - E_t(\text{AlN}) - \mu_O + \mu_{Al} + \mu_N + q\varepsilon_F + \Delta^q, \quad (1)$$

where $E_t[(V_{Al}\text{–}O_N)^q]$ is the total energy of the supercell containing a V_{Al}-O_N complex in charge state q and E_t(AlN) is the total energy of a perfect crystal in the same supercell.

The Al atom removed from the crystal is placed in a reservoir of energy μ_{Al}, and the N atom that is removed is placed in a reservoir of energy μ_N. The chemical potentials μ_{Al} and μ_N are referenced to the energy per atom of Al bulk and N_2 molecules, and can vary over a range determined by the calculated formation enthalpy of AlN [$\Delta H_f(\text{AlN}) = -3.18$ eV], reflecting growth conditions all the way from Al-rich to N-rich. The oxygen atom is taken from a reservoir with energy μ_O, referenced to the energy per atom of the O_2 molecule. We assume the chemical potential of oxygen is limited by the formation of Al_2O_3, with a calculated formation enthalpy of $\Delta H_f(Al_2O_3) = -16.2$ eV. The upper limit of μ_O is then determined by $2\mu_{Al} + 3\mu_O = \Delta H_f(Al_2O_3)$. In the case of charged defects, electrons are exchanged with the reservoir for electrons in the solid, the energy of which is the Fermi level ε_F, referenced to the valence-band maximum (VBM). The last term in Eq. (1), Δ^q, is the correction for charged defects due to the finite size of the supercell, as described in Refs. 32 and 33.

When forming an Al vacancy, the removal of the Al atom results in four N dangling bonds. In the near-tetrahedral environment of the wurtzite structure, these p-like states are split in a singlet and a triplet state. In the neutral charge state, these states are occupied by a total of three electrons. By successively adding electrons to the Kohn-Sham states of the defect, 1−, 2−, and 3− charge states may be obtained. Addition of electrons to the vacancy results in an outward breathing relaxation: In the 3− charge state, the three equivalent nitrogen atoms move outward by 11% of the perfect-crystal bond length, while the N atom along the c axis moves outward by 16%.

The association of V_{Al} and O_N, resulting in a V_{Al}-O_N complex, involves an electron transfer from the O_N to the V_{Al}. Since oxygen p states are lower in energy than nitrogen p states, the defect states will move closer to the VBM. The local lattice relaxations for the $(V_{Al}\text{-}O_N)^{2-}$ complex are illustrated in Fig. 1(a). The three nearest-neighbor N atoms are displaced away from the vacancy by 9.3% and 9.1% of the equilibrium Al-N bond length in the 2− and 1− charge states; the O atom along the c-axis relaxes away from the vacancy by 14.1% and 13.9% in the 2− and 1− charge states, respectively.

As shown in Fig. 2, the V_{Al} has a low formation energy when the Fermi level is in the upper part of the band gap, where it is stable in a 3− charge state. The 2−/3− thermodynamic transition level is located at 3.11 eV above the VBM. Similarly, the V_{Al}-O_N complex is most stable for ε_F values high in the gap, with a charge state of 2−; the −/2− transition level occurs at 2.59 eV above the VBM. The choice of Al_2O_3 as the solubility-limiting phase introduces a dependence of the formation energy of V_{Al}-O_N on the host chemical potentials. Consequently, V_{Al}-O_N has lower formation energy in N-rich than in Al-rich conditions. V_{Al}-O_N complexes have lower formation energy than isolated vacancies for most Fermi-level positions within the band gap, under both Al-rich and N-rich conditions. The binding energy (E_b) of the $(V_{Al}\text{-}O_N)^{2-}$ complex with respect to dissociation into O_N^+ and V_{Al}^{3-} is 1.12 eV, indicating that there is indeed a strong driving force for Al vacancies and oxygen impurities to form complexes. The formation energies of V_{Al} and related complexes may be somewhat underestimated due to the underestimation of the magnitude of the enthalpy of

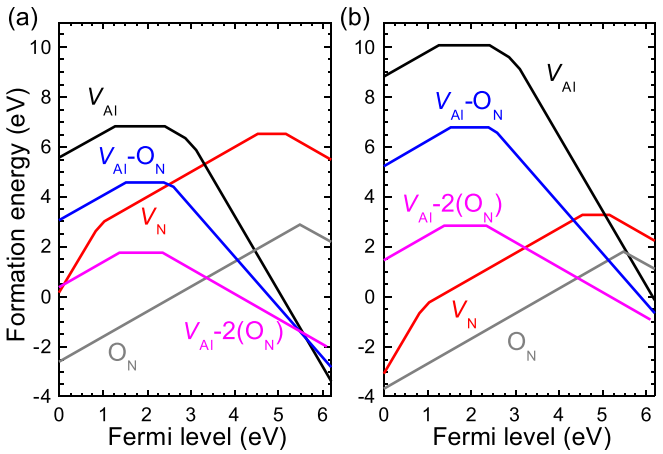

FIG. 2. Formation energies as a function of Fermi level for the nitrogen vacancy V_N, aluminum vacancy V_{Al}, oxygen impurity O_N, and vacancy-oxygen complexes V_{Al}-O_N and V_{Al}-2(O_N), under (a) N-rich and (b) Al-rich conditions.

formation in our calculations. The formation energies of oxygen-related species are low, consistent with the tendency for oxygen incorporation in AlN, but note that the values in Fig. 2 assume the oxygen chemical potential corresponds to the solubility limit, i.e., equilibrium with Al_2O_3; realistic conditions of unintentional oxygen incorporation would lead to higher formation energies.

The kinks in the curves of Fig. 2 correspond to thermodynamic transition levels; these levels are summarized in Fig. 1(b). All of these defects potentially lead to characteristic absorption and emission peaks. The optical transition energies are determined from the configuration-coordinate diagrams shown in Fig. 3. The energy difference between minima of the two curves in such diagrams corresponds to the zero-phonon line and is equal to the energy difference between the $q/q+1$ transition level (Fig. 2) and the conduction-band minimum (CBM) [for transitions involving electrons in the conduction band (CB)] or the VBM [for transitions involving holes in the valence band (VB)]. The local lattice relaxations are quite different for different charge states and lead to significant Stokes shifts and strong vibrational broadening of absorption and emission peaks.

In the absence of intentional doping, the Fermi level is most likely to occur in the upper part of the band gap, because of the tendency of the material to incorporate donor-type impurities, particularly oxygen. When the Fermi level is above 3.11 eV (in the case of V_{Al}) or above 2.59 eV (for V_{Al}-O_N), the defect states of both V_{Al} and V_{Al}-O_N are fully occupied. Optical absorption can therefore involve only transitions from occupied defect states to empty CB states (or shallow donors). The peak absorption energy corresponds to the energy difference between V_{Al}^{3-} as the initial state and V_{Al}^{2-} fixed in the lattice configuration of V_{Al}^{3-} as the final state. This results in an absorption peak at 3.43 eV, with a relaxation energy of 0.34 eV as shown in Fig. 3(a). This peak agrees very well with the absorption peak observed at around 3.4 eV in irradiated samples.[4,13] This absorption band was previously attributed to the nitrogen vacancy.[13] However, our calculations show that all band-to-defect and defect-to-band absorption peaks involving V_N in 0, +, or 3+ charge states are either higher than 5.1 eV or lower than 2.3 eV, which rules out the possibility that the nitrogen vacancy is responsible for the 3.4 eV absorption peak. We can therefore attribute this absorption peak to V_{Al} formed during irradiation.

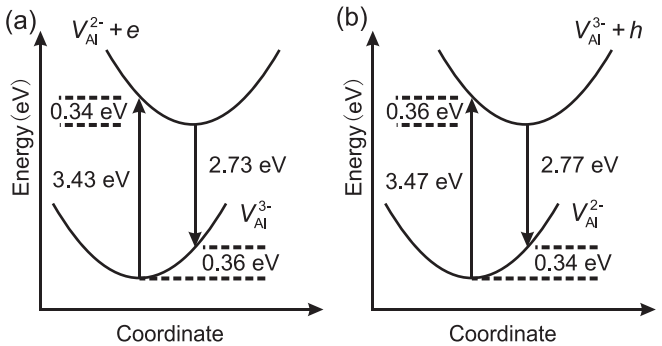

FIG. 3. Configuration-coordinate diagrams for V_{Al}. (a) Transition between an electron in the deep acceptor state and the CBM. (b) Transition between the deep acceptor state and a hole in the VBM.

Another broad absorption band which is frequently observed in oxygen-containing AlN samples is centered around 2.9 eV. Inspection of the defects and complexes shown in Fig. 2 indicates that none of the defects or complexes studied here absorbs in this range. One possibility is that two different defects are involved in this transition. Assuming the Fermi level is located in the upper part of the band gap, V_{Al}-O_N should be in a 2− charge state, while V_N can be in a +, 0, 1−, or 2− charge state. The negatively charged nitrogen vacancies are unlikely to bind to V_{Al}-O_N due to the repulsive electrostatic interaction. Assuming a V_N in a + charge state is in the vicinity of a V_{Al}-O_N in a 2− charge state, an electron excited from V_{Al}-O_N can be transferred to V_N $[(V_{Al}-O_N)^{2-}+V_N^{+}\rightarrow(V_{Al}-O_N)^{-}+V_N^{0}]$. By adding the relaxation energies of both V_N and V_{Al}-O_N to the difference in ionization energies of these two vacancies in their original charge states, we obtain an absorption peak at 3.03 eV, in good agreement with the absorption peak observed at 2.9 eV. Another candidate would be a transition involving the bare V_{Al} and V_N: depending on the charge state of V_N, the approach outlined above would lead to absorption peaks at 2.49 eV $(V_{Al}^{3-}+V_N^{+}\rightarrow V_{Al}^{2-}+V_N^{0})$ or 3.07 eV $(V_{Al}^{3-}+V_N^{0}\rightarrow V_{Al}^{2-}+V_N^{-})$. Explicit binding between the defects, not taken into account in these estimates, could shift these values to some extent. Hence, any of these inter-defect-transitions between V_{Al} and V_N could be responsible for the broad absorption at 2.9 eV. We are aware, however, that the Fermi-level positions required for our proposed transitions are not necessarily those that occur in some of the experimental observations,[9] and our proposed mechanism is therefore clearly not the only one to give rise to 2.9 eV absorption.

Let us now turn to luminescence. After excitation has taken place, the electron in the conduction band can recombine with a hole in the defect state, leading to optical emission. For V_{Al}^{2-}, this results in an emission peak at 2.73 eV, with a relaxation energy of 0.36 eV [Fig. 3(a)]. In reality, the efficiency of this process may be limited due to the scattering of conduction electrons by negatively charged defects. Another emission process is more likely: during optical excitation, holes are generated in the VB and transitions of electrons from the defect state to the VB become possible. Negatively charged vacancies actually act as attractive centers for holes. The $(V_{Al})^{3-}+h\rightarrow(V_{Al})^{2-}$ process results in an emission peak at 2.77 eV, as shown in Fig. 3(b). The absorption and emission energies involving the VB (Fig. 3(b)] turn out to be very close to the values for transitions involving the CB [Fig. 3(a)], due to the fact that the 2−/3− thermodynamic transition level is near mid-gap [Fig. 1(b)]. The calculated emission peak agrees very well with the observed photoluminescence band centered around 2.78 eV in AlN samples with relatively low oxygen concentrations $(2\times10^{18}\,cm^{-3})$.[12] Such samples are more likely to contain isolated V_{Al} defects, while V_{Al}-O_N complexes are likely to be more prevalent in samples with higher oxygen concentrations.

A recent paper,[25] assigned the emission peak at 2.8 eV in carbon-doped AlN to a V_N-C_N complex, based on a

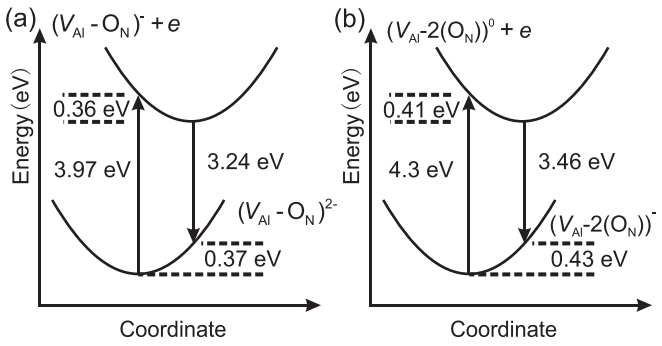

FIG. 4. (a) Configuration-coordinate diagram for V_{Al}-O_N for the transition between an electron in the deep acceptor state and the CBM. (b) Configuration-coordinate diagram for V_{Al}-2(O_N) for the transition between an electron in the deep acceptor state and the CBM.

donor-acceptor-pair (DAP) model. However, the energies used in the DAP model in Ref. 25 were the thermodynamic transition energies of V_N and C_N, without the inclusion of relaxation effects that are necessary to get accurate optical transition energies. The presence of strong coupling with the lattice is evident from the fact that the observed 2.8 eV PL signal is very broad. In addition, the DAP model used is not appropriate for deep levels with strongly localized wave functions.

Figure 4 illustrates the transitions associated with the V_{Al}-O_N complex. The electron excited in the CB can recombine with a hole in the defect state, resulting in an emission peak at 3.24 eV, with a relaxation energy of 0.37 eV [Fig. 4(a)]. We therefore assign the luminescence band centered around 3.1–3.3 eV observed in oxygen-containing samples[14–16] to a transition involving an electron in the CB with $(V_{Al}\text{-}O_N)^-$. The transition $(V_{Al}\text{-}O_N)^{2-} \rightarrow (V_{Al}\text{-}O_N)^- + e$ gives rise to an optical absorption peak at 3.97 eV, with a relaxation energy of 0.36 eV [Fig. 4(a)]. This indicates that the V_{Al}-O_N complex is a source of the absorption band around 4.0 eV observed in as-grown AlN bulk crystals, which have oxygen concentrations higher than $10^{19}\,cm^{-3}$ (Refs. 8 and 9). Note that the observed absorption peak at around 4.0 eV is very broad and the peak position varies in samples with different oxygen concentrations.[9] We propose that several oxygen-related defect complexes, including V_{Al}-O_N, V_{Al}–2(O_N), and possibly V_{Al}–3(O_N), are present in the samples and responsible for the broadness of the absorption peak. Support for this scenario is provided by our calculations, which reveal that the transition $(V_{Al}\text{–}2(O_N))^- \rightarrow (V_{Al}\text{–}2(O_N))^0 + e$ gives rise to an optical absorption peak at 4.3 eV, with a relaxation energy of 0.41 eV [Fig. 4(b)]. Furthermore, as shown in Fig. 4(b), we find an emission peak involving a transition from the CBM to the defect state of V_{Al}–2(O_N) at 3.46 eV, which is in good agreement with the 3.6 eV emission peak observed experimentally.[17–19] We thus propose V_{Al}–2(O_N) as the main source of this emission peak. The fact that the width and peak position of the 3.6 eV emission band is sample dependent may again be associated with it consisting of several overlapping bands involving V_{Al}-O_N, V_{Al}–2(O_N), and possibly V_{Al}–3(O_N).

In summary, using hybrid density functional calculations we have shown that isolated aluminum vacancies can explain the absorption peak at 3.4 eV observed in irradiated AlN samples, and the luminescence signal at 2.8 eV observed in AlN containing low concentrations of oxygen impurities. Complexes of an aluminum vacancy and oxygen impurities give rise to absorption peaked at 4.0 eV or higher, depending on the oxygen concentration, and emission peaked at 3.2–3.5 eV, explaining the absorption and luminescence bands observed in AlN containing high levels of oxygen impurities. The broad absorption band centered around 2.9 eV is suggested to be due to a transition between V_{Al} [or $(V_{Al}\text{-}O_N)$] and V_N.

This work was supported by the Center for Low Energy Systems Technology (LEAST), one of the six SRC STARnet Centers, sponsored by MARCO and DARPA, and by the UCSB Solid State Lighting and Energy Center. We thank M. Bickermann, J. Lyons, and L. Gordon for fruitful discussions. Computing resources were provided by CSC/CNSI/MRL (NSF-CNS-0960316) and XSEDE (NSF-DMR-070072N).

[1]R. Schlesser, R. Dalmau, and Z. Sitar, J. Cryst. Growth **241**, 416 (2002).
[2]J. C. Rojo, G. A. Slack, K. Morgan, B. Raghothamachar, M. Dudley, and L. J. Schowalter, J. Cryst. Growth **231**, 317 (2001).
[3]G. A. Slack, R. A. Tanzilli, R. O. Pohl, and J. W. Vandersande, J. Phys. Chem. Solids **48**, 641 (1987).
[4]J.-M. Mäki, I. Makkonen, F. Tuomisto, A. Karjalainen, S. Suihkonen, J. Räisänen, T. Y. Chemekova, and Y. N. Makarov, Phys. Rev. B **84**, 081204 (2011).
[5]S. M. Evans, N. C. Giles, L. E. Halliburton, G. A. Slack, S. B. Schujman, and L. J. Schowalter, Appl. Phys. Lett. **88**, 062112 (2006).
[6]N. T. Son, A. Gali, A. Szabó, M. Bickermann, T. Ohshima, J. Isoya, and E. Janzén, Appl. Phys. Lett. **98**, 242116 (2011).
[7]G. A. Slack and T. F. McNelly, J. Cryst. Growth **42**, 560 (1977).
[8]G. A. Slack, L. J. Schowalter, D. Morelli, and J. A. Freitas, Jr., J. Cryst. Growth **246**, 287 (2002).
[9]M. Bickermann, B. M. Epelbaum, and A. Winnacker, J. Cryst. Growth **269**, 432 (2004).
[10]M. Bickermann, A. Münch, B. M. Epelbaum, O. Filip, P. Heimann, S. Nagata, and A. Winnacker, J. Appl. Phys. **103**, 073522 (2008).
[11]G. A. Cox, D. O. Cummins, K. Kawabe, and R. H. Tredgold, J. Phys. Chem. Solids **28**, 543 (1967).
[12]A. Sedhain, L. Du, J. H. Edgar, J. Y. Lin, and H. X. Jiang, Appl. Phys. Lett. **95**, 262104 (2009).
[13]K. Atobe, M. Honda, N. Fukuoka, M. Okada, and M. Nakagawa, Jpn. J. Appl. Phys., Part 1 **29**, 150 (1990).
[14]R. A. Youngman and J. H. Harris, J. Am. Ceram. Soc. **73**, 3238 (1990).
[15]M. Morita, K. Tsubouchi, and N. Mikoshiba, Jpn. J. Appl. Phys., Part 1 **21**, 1102 (1982).
[16]T. Koyama, M. Sugawara, T. Hoshi, A. Uedono, J. F. Kaeding, R. Sharma, S. Nakamura, and S. F. Chichibu, Appl. Phys. Lett. **90**, 241914 (2007).
[17]M. Strassburg, J. Senawiratne, N. Dietz, U. Haboeck, A. Hoffmann, V. Noveski, R. Dalmau, R. Schlesser, and Z. Sitar, J. Appl. Phys. **96**, 5870 (2004).
[18]M. Bickermann, B. M. Epelbaum, O. Filip, P. Heimann, S. Nagata, and A. Winnacker, Phys. Status Solidi B **246**, 1181 (2009).
[19]T. Schulz, M. Albrecht, K. Irmscher, C. Hartmann, J. Wollweber, and R. Fornari, Phys. Status Solidi B **248**, 1513 (2011).
[20]T. Mattila and R. M. Nieminen, Phys. Rev. B **55**, 9571 (1997).
[21]I. Gorczyca, A. Svane, and N. E. Christensen, Phys. Rev. B **60**, 8147 (1999).
[22]C. Stampfl and C. G. Van de Walle, Phys. Rev. B **65**, 155212 (2002).
[23]C. G. Van de Walle and J. Neugebauer, J. Appl. Phys. **95**, 3851 (2004).
[24]K. Laaksonen, M. G. Ganchenkova, and R. M. Nieminen, J. Phys.: Condens. Matter **21**, 015803 (2009).
[25]B. E. Gaddy, Z. Bryan, I. Bryan, R. Kirste, J. Xie, R. Dalmau, B. Moody, Y. Kumagai, T. Nagashima, Y. Kubota *et al.*, Appl. Phys. Lett. **103**, 161901 (2013).
[26]W. Kohn and L. J. Sham, Phys. Rev. **140**, A1133 (1965).
[27]G. Kresse and D. Joubert, Phys. Rev. B **59**, 1758 (1999).
[28]P. E. Blöchl, Phys. Rev. B **50**, 17953 (1994).

[29]J. Heyd, G. E. Scuseria, and M. Ernzerhof, J. Chem. Phys. **118**, 8207 (2003).
[30]J. Heyd, G. E. Scuseria, and M. Ernzerhof, J. Chem. Phys. **124**, 219906 (2006).
[31]G. Kresse and J. Furthmüller, Phys. Rev. B **54**, 11169 (1996).
[32]C. Freysoldt, J. Neugebauer, and C. G. Van de Walle, Phys. Rev. Lett. **102**, 016402 (2009).
[33]C. Freysoldt, J. Neugebauer, and C. G. Van de Walle, Phys. Status Solidi B **248**, 1067 (2011).